Available online at www.sciencedirect.com

ScienceDirect

Energy Procedia 80 (2015) 30 – 37

Energy Procedia

12th Deep Sea Offshore Wind R&D Conference, EERA DeepWind'2015

A fast reduced order method for assessment of wind farm layouts

Yngve Heggelund[a,*], Chad Jarvis[a], Marwan Khalil[b]

[a]*Christian Michelsen Reseach AS, NO-5892 Bergen, Norway*
[b]*GexCon AS, NO-5892 Bergen, Norway*

Abstract

Due to wake losses, the power production of wind farms depend on the positioning of turbines in relation to each other, i.e. the wind farm layout. Computational Fluid Dynamics (CFD) can be used for solving the complex flow in a wind farm since wake effects are inherently simulated. However, it is too slow for interactively assessing the power production for variations of wind farm layouts. Therefore, there is a need for an accurate and fast model based on CFD for computing the flow field and the wake losses in a wind farm for a range of wind speeds and wind directions. In this paper, we adapt model reduction methodology to wind farm flow. The governing equations are formulated in a reduced finite dimensional space spanned by a set of orthogonal modes created from CFD simulations. The accuracy of the reduced model is assessed on a set of test cases. In the reduced model, new solutions for different turbine layouts and wind speeds are produced in a matter of seconds, as opposed to hours for full CFD simulations.

Peer-review under responsibility of SINTEF Energi AS

Keywords: Wind farm layout; offshore wind; model reduction; CFD

1. Introduction

Offshore wind power is increasingly becoming more important as a renewable energy source and large investments in offshore wind farm projects are expected in near future.

Power losses from wakes in wind farms are difficult to predict, and the impact on power production from underestimation of the wake effect has been estimated to be in the region of 5-10% [1]. There is a need for fast and

* Corresponding author. Tel.: +47 917 97 224; fax: +47 55 57 40 41.
E-mail address: yngve@cmr.no

Peer-review under responsibility of SINTEF Energi AS
doi:10.1016/j.egypro.2015.11.403

accurate methods for evaluation of power production to enable interactive design and optimization of wind farm layouts.

This study uses the power production as the layout design parameter, where layout refers to the number and positioning of turbines within the wind farm area. There are clearly other parameters to consider such as fatigue loads, sea bed conditions and the electrical system, but the power production is considered the dominant layout design parameter [2].

The current state-of-the-art is to use simplified models for the turbine wakes since they are computationally fast. Many different wake models exist and are in use in commercial wind resource software such as WaSP (www.wasp.dk), WindPro (www.emd.dk/WindPRO) and GH WindFarmer (www.gl-garradhassan.com). The Jensen model [3] is probably the first wake model proposed. The model is based on a linear expansion of the wake region, and mass conservation. Since then, several other simplified models have been introduced. For example, the Frandsen model [4] and the Ainslie model [5]. Studies have been performed comparing many of these wake models in an offshore setting (see for example [6]). From these studies, no particular model seems to outperform the other models. In large wind farms, these wake models appear to under-predict wake losses [7].

Computational Fluid Dynamics (CFD) is a powerful tool, which can be used for solving the complex flow in a wind farm since wake effects are inherently simulated. CFD is, however, computationally expensive, which makes it unsuitable in an interactive design tool where the user expects fast response. This leads to the investigation of alternative CFD based techniques for solving the wind farm flow. Fuga [8] is a promising linearized CFD model for offshore wind farms. The model performs several orders of magnitude faster than the standard CFD simulation. However, since it is linearized it is not clear that it captures all the necessary physics of the flow in a wind farm.

The approach investigated here is a CFD based approach using a model reduction technique of the steady state Reynolds Averaged Navier-Stokes (RANS) equations. This approach rather than simplifying the RANS equations simplifies the solution space and still includes the nonlinear effects. Model reduction is a technique which has successfully been applied to CFD models within other areas of application, e.g. study of flow past a rectangular cavity [9], compressible flows [10], optimal rotary control of cylinder wake [11], and computer graphics [12], [13]. Other examples include weather forecasting, image processing, signal analysis and data compression [14]. To our knowledge model reduction has not yet been applied to wind farm flow using steady state RANS.

2. Theoretical framework

The idea of model reduction is to formulate the governing equations in a reduced finite dimensional solution space spanned by a set of orthogonal basis modes. For three-dimensional grids, the modes are cell values arranged in one-dimensional vectors by some pre-determined ordering.

2.1. Reduced order model

The governing equations considered here are the steady state RANS equations with the k-ε turbulence closure scheme. Using Einstein notation the momentum equations are given by

$$\rho \frac{\partial}{\partial x_j}\left(u_i u_j\right) = -\frac{\partial p}{\partial x_i} + \frac{\partial}{\partial x_j}\left(\sigma_{ij}\right), \tag{1}$$

where the stress tensor σ_{ij} is given by

$$\sigma_{ij} = \mu\left(\frac{\partial u_i}{\partial x_j} + \frac{\partial u_j}{\partial x_i}\right) - \frac{2}{3}\delta_{ij}\rho k. \tag{2}$$

The density ρ is assumed constant, and the flow is incompressible and divergence free.

In discretized form, these equations can be expressed as matrices applied to state vectors. Given a state vector $\boldsymbol{q}$ consisting of the three velocity components the pressure, the turbulent kinetic energy, and the effective viscosity, the discretized version of the steady state incompressible RANS momentum equations may be written

$$\left(A_q + P - V_q - K\right)\boldsymbol{q} = 0. \quad (3)$$

The matrices A_q, P, V_q and K are large sparse matrix representations of the operators for the advection term, pressure term, viscosity term, and turbulent kinetic energy term respectively. The subscript q on the nonlinear advection and viscosity matrix operators denotes that they depend linearly on the state vector $\boldsymbol{q}$.

Let $\boldsymbol{a}^{\mathrm{T}} = [a_1, a_2, \cdots, a_{\mathrm{M}}]$, where M is much less than the number of grid cells N in the CFD solution, be a vector of coefficients which represent the state in the reduced space. Then, the reconstructed state in the full space may be expressed as

$$\boldsymbol{q} = \sum_{m=1}^{M} a_m \boldsymbol{\varphi}_m = B\boldsymbol{a}, \quad (4)$$

where $\mathrm{B} = [\boldsymbol{\varphi}_1, \boldsymbol{\varphi}_2, \cdots, \boldsymbol{\varphi}_{\mathrm{M}}] \in \mathbb{R}^{6\mathrm{N}\times\mathrm{M}}$ is the matrix containing the basis vectors. Inserting this into equation 3 and using Galerkin projection onto the reduced space (left-multiplying by B^T) results in the equation

$$\left(\sum_{m=1}^{M} a_m B^T\left(A_{\varphi_m} - V_{\varphi_m}\right) B + B^T(P - K)B\right)\boldsymbol{a} = \boldsymbol{0}. \quad (5)$$

Equation 5 is a reduced order model of the steady state RANS momentum equations. The fulfillment of this equation is used as a constraint to avoid non-physical solutions (see section 2.4). In practice, we look for the values of the coefficient vector $\boldsymbol{a}$ that minimizes the left hand side of equation 5.

Since the reduced space is much smaller than the full space, evaluation of a solution in the reduced space is much faster.

2.2. Construction of basis

The construction of a lower dimensional representative basis is a critical step in model reduction. The basis must be large enough to span the most significant possible solutions, while at the same time be sufficiently small to enable fast computation times.

A common approach for constructing the basis is the method of snapshots [14], [9], combined with Proper Orthogonal Decomposition (POD). Snapshots are typically produced by running CFD simulations, and extracting the solution for different boundary conditions and at different time steps (if the phenomenon is time-dependent). From this set of snapshots, an orthonormal basis can be constructed by applying Singular Value Decomposition (SVD), which has the property that the left singular vectors span the same space as the snapshots, are orthonormal and sorted according to their significance with respect to reproducing the snapshot set. If the snapshots are linearly independent, the number of basis vectors will be equal to the number of snapshots. Typically, many snapshots are produced and the most significant left singular vectors from SVD to are kept to form the basis. These vectors are also known as the POD modes. It is important that the snapshots produced are representative for the cases to be studied so that the basis is suitable for reconstructing the actual flow fields.

2.3. Tiling

We capture localized behavior around each wind turbine by introducing tiles around each of them. A tile is a three-dimensional region with fixed size containing either a wind turbine at a fixed position related to the box boundaries

or no wind turbine. We call these turbine tiles and empty tiles respectively. Complete wind farms can be assembled interactively in real time from turbine tiles and empty tiles, see Fig 1.

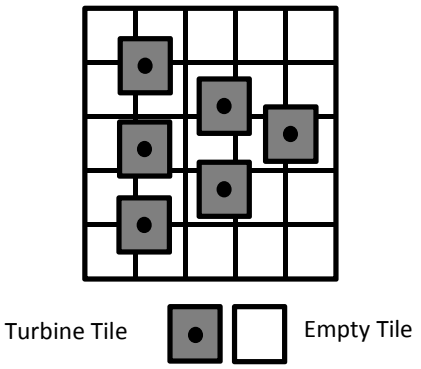

Fig 1 Assembling a wind farm from tiles containing turbines with empty tiles in between.

In principle, each tile can have its own basis. However, in this paper we use one common basis for turbine tiles and another common basis for empty tiles.

2.4. The combined objective function

The overall best solution minimizes the discrepancy of the boundary values both between tiles and to external conditions, while at the same time minimizes the discrepancy to the RANS momentum equations.

Boundary fitting is a minimization problem. A least squares method is used, which can be shown to have the form

$$\mathrm{F}(\boldsymbol{x}) = \tfrac{1}{2}\|A\boldsymbol{x} - \boldsymbol{b}\|_2^2, \quad (6)$$

where x is a compound vector of the reduced space solution of all the tiles which share boundaries.

The objective function C(x) for fitting the solutions at tile boundaries has the form

$$\mathrm{C}(\mathbf{x}) = \frac{1}{2}\big[\,(1-\alpha)\mathrm{F}(\mathbf{x}) + \alpha\mathrm{R}(\mathbf{x})\big], \quad (7)$$

where α is a scalar between 0 and 1, F(x) is the boundary fitting function (derived in [15]), and R(x) is the function for the steady state incompressible RANS equations (see the left hand side of equation 5). The choice of α represents a compromise between the boundary discrepancies and the momentum discrepancies.

3. Results

We have utilized the CFD simulator CMR-Wind [16, 17, 18, 19] for solving the transient RANS equations, and generating the basis for the tiles. For the first test case we use a turbine of type BONUS MK III 450 kW with a hub height of 50 m and a rotor diameter of 37 m, while for the other test cases we use a turbine of type BONUS 2MW with a hub height of 64 m and a rotor diameter of 76 m. The inflow wind field for all the test cases is a neutrally stratified flow over a surface of roughness length of 3 cm.

The power production of a wind turbine typically starts at the so-called cut-in speed and increases as a function of the wind speed cubed until some point where the blades are adjusted to limit the power production to a maximal level. A cubic relationship between power and wind speed means that any relative discrepancy in the wind speed will have three times the effect on the relative discrepancy of the power.

For all the test cases in this report, it takes less than a second to compute a solution on a four core desktop computer.

3.1. Crosswind movement of turbines

The first test case is an idealized three-turbine system with wind from the west having two turbines at fixed positions in the front and one turbine to be positioned downstream, see Fig 2 (left). The inflow wind speed at hub height is 7 m/s.

The front tiles and the downstream tile all share the same basis. We generate six CFD simulations for different crosswind positions of the backmost turbine (turbine C), by moving the turbine from the center position (0 m) up to 75 m along the vertical axis. From these simulations for each tile we extract five snapshots above the center position, five mirror snapshots below the center position, and one snapshot from the center position, for a total of 11 snapshots for each tile, giving 33 snapshots in total. From these snapshots, we use SVD to create two bases, one with the five most significant modes, and one with the 15 most significant modes.

We then compute solutions with model reduction of the flow field for 30 equidistant positions of the downstream turbine (C) between the center position to directly behind turbine B. To investigate the sensitivity of the results to the number of basis modes, we compute results using five and 15 basis modes. Fig 2 (right) shows the resulting power production of turbine C as a function of its crosswind position. The eleven red points (square and circular) show the results from full CFD simulations. The six square points correspond to the snapshots used to build the basis and the remaining five circular points are independent control points. Using 15 basis modes seems to be sufficient to represent the flow features needed for production estimation. Additionally, the production estimates for five modes in the basis also show a reasonably good approximation of the results produced by CFD simulator.

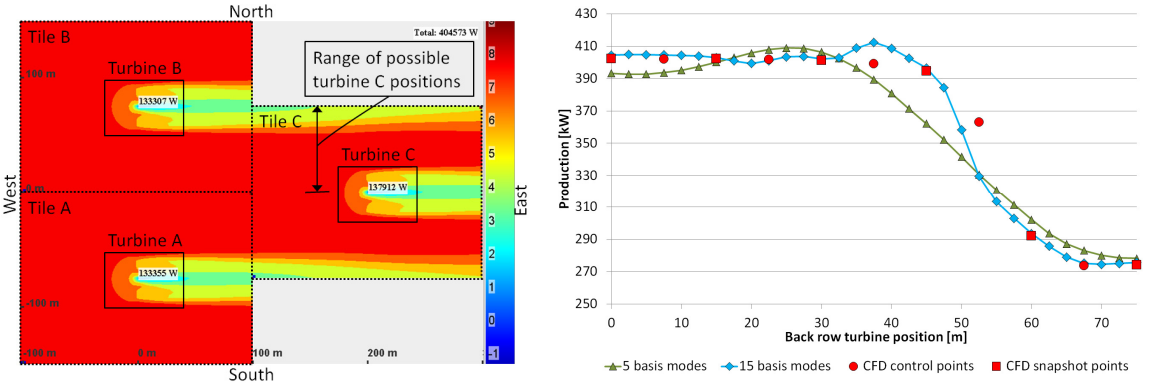

Fig 2. (Left) solution of the x-component of the flow field (m/s) at hub-height for optimal position of turbine C with respect to power production, using 15 basis modes and an α of 0.5. (Right) Production estimates for the wind farm for different positions of turbine C. The value 0 m refers to a position at the midpoint between the two front row turbines, and 75 m refers to a position directly behind turbine B.

3.2. Line setups with varying downstream distances

The next test case consists of ten turbines in a line, where we uniformly vary the downstream distances between them. We build the basis from CFD simulations with turbine distances of five and nine rotor diameters (380 m and 684 m). The inflow wind speed at hub height is 7 m/s. The snapshots used for the basis construction had to have the

same dimensions, so consequently there is an overlap of the snapshots extracted from the five rotor diameter case as illustrated in Fig 3.

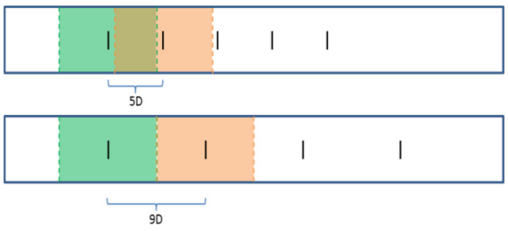

Fig 3 Snapshot extraction from simulations with turbine distances of five and nine rotor diameters.

We constructed the basis from CFD simulations with less than ten turbines. An equal number of snapshots from the five and nine rotor diameter cases are used to construct the basis, for example three snapshots from the five diameter case and three snapshots from the nine diameter case (which we label as 3 + 3 modes).

Fig 4 shows comparisons of the model reduction results to results simulated with CFD for cases with turbine distances of six, seven and eight rotor diameters. The total deviation of the power production between the model reduction and the CFD result is less than 3.3% when using 4 + 4 or more modes. Some additional results for this test case are reported in [20] and [21].

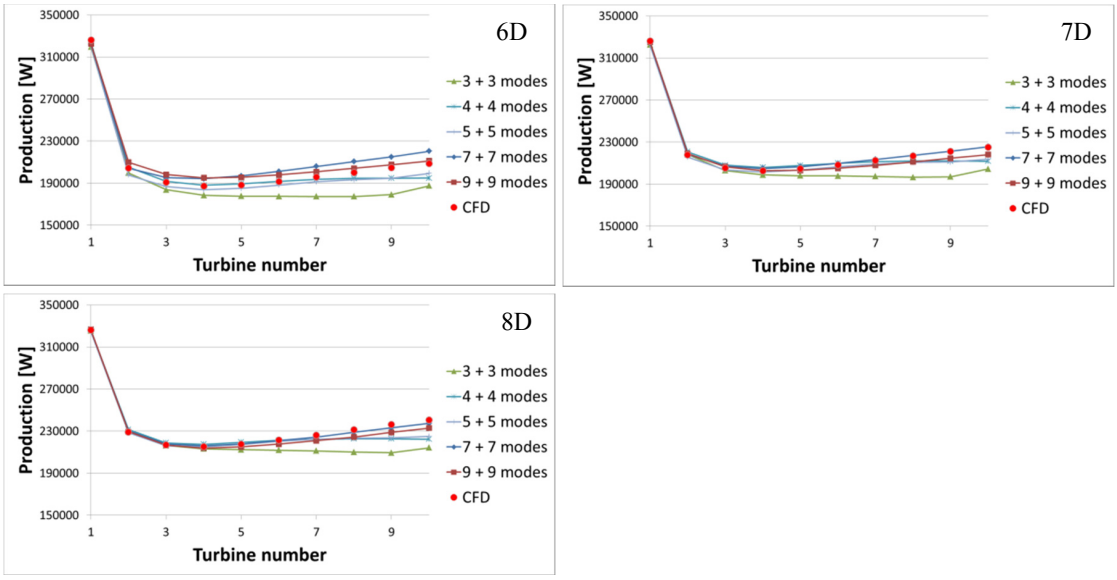

Fig 4 The power production for the six rotor diameter case (6D), the seven rotor diameter case (7D) and the eight rotor diameter case (8D) as a function of the turbine number for different basis sizes. We constructed the basis using an equal number of snapshots from simulations with five and nine rotor diameter distances.

3.3. Varying wind speeds

For the last test case, we study the behavior for different wind speeds in neutrally stratified flow. We consider fixed turbine positions in a layout as illustrated in Fig 5, and we simulated the setup with CFD for wind speeds at hub height of 7 m/s, 9 m/s, 11 m/s, 13 m/s, and 15 m/s. The simulations of 9 m/s, and 13 m/s wind speed are not used to construct the basis, but for assessing the model reduction results. We study how well model reduction can reproduce the turbine productions for these wind speeds using a basis constructed from a subset of these simulations.

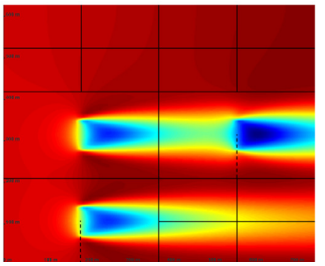

Fig 5 Test setup for the wind speed study. The downstream turbine is placed five rotor diameters downstream of the two upstream turbines. The distance between the two upstream turbines is 2.75 rotor diameters. The black lines show the outline of the tiles.

Naturally, the production of the downstream turbine has the highest discrepancy between the model reduction results and the CFD results. We therefore focus our attention on the production of the downstream turbine as a function of the simulations used to produce the bases and the scalar α, defined in section 2.4. Fig 6 shows the relative discrepancy of the power production of the downstream turbine. As can be seen, the dependency on α is weaker when the basis is constructed from simulations of 7, 11 and 15 m/s as opposed to only 7 and 15 m/s. In our experience the value of α should not be close to the extreme values. Here we see that the discrepancy increases rapidly as α approaches 1. In earlier studies, we have observed similar behavior as α approaches 0.

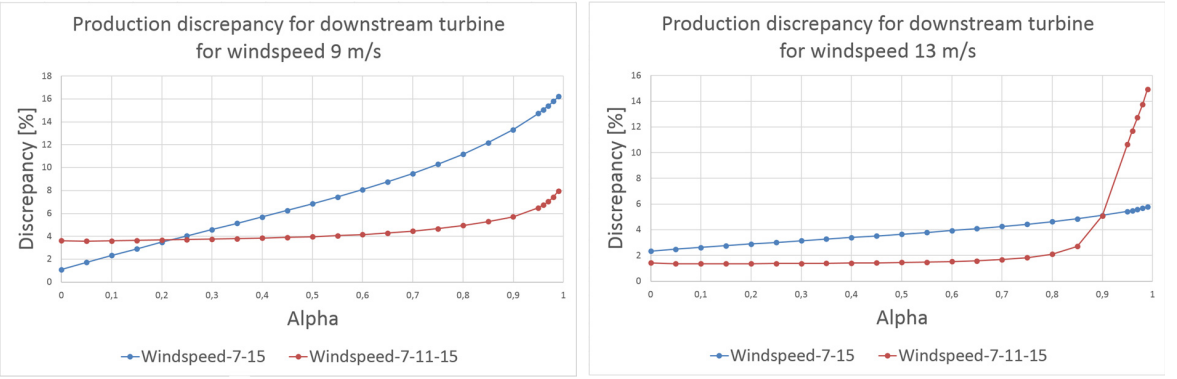

Fig 6 The discrepancy as a function of α for wind speed 9 m/s (left) and 13 m/s (right). The blue curve is for a basis constructed from CFD simulations of wind speeds 7 m/s and 15 m/s, while the red curve is for a basis constructed from CFD simulations of wind speeds 7 m/s, 11 m/s and 15 m/s.

4. Concluding remarks

We have presented a model reduction technique based on CFD for fast flow field computation in wind farms. The model reduction technique is implemented by a trade-off objective function between boundary-coupling of tiles and the steady state RANS momentum balance. With this proposed model reduction approach results are computed within seconds rather than several hours using CFD simulations.

The model reduction technique is able to simulate the effect of many interacting wakes from a relatively small set of underlying CFD simulations. For three different test cases, the power production from CFD agrees well with the model reduction results. All the test cases take less than one second to compute. This shows that once a basis is constructed, using the model reduction technique saves significant computing time compared to CFD simulations, without large sacrifices to the accuracy. We plan to scale the verification studies to larger wind farms in the near future.

References

[1] European Wind Energy Technology Platform. “Strategic research agenda: market deployment strategy from 2008 to 2030”, July 2008. Available online: http://www.windplatform.eu/fileadmin/ewetp_docs/Bibliography/SRA_MDS_July_2008.pdf
[2] Wind Energy - The Facts - A guide to the technology, economics and future of wind power. European Wind Energy Association, Earthscan 2009. (http://www.wind-energy-the-facts.org/).
[3] Jensen NO (1983) A note on wind generator interaction. Risø M 2411. Risø National Laboratory, Roskilde (Denmark).
[4] Frandsen S, Barthelmie RJ, Pryor S, Rathmann O, Larsen S, Højstrup J, Thøgersen M (2006). Analytical modelling of wind speed deficit in large offshore wind farms. Wind Energy 9(1-2): 39-53.
[5] Ainslie JF (1988). Calculating the flowfield in the wake of wind turbines. Journal of Wind Engineering and Industrial Aerodynamics 1988; 27: 213-224.
[6] Rados K, Larsen G, Barthelmie R, Schlez W, Lange B, Schepers G, Hegberg T, Magnisson M (2002). Comparison of wake models with data for offshore windfarms. Wind Engineering, 2002. 25: p. 271-280.
[7] Mechali M, Barthelmie R, Frandsen S, Jensen L, Réthoré P-E (2006). Wake effects at Horns Rev and their influence on energy production. in EWEC 2006. Athens, Greece: p. 10.
[8] Ott S, Berg J, Nielsen M (2011). Linearised CFD models for wakes. Risø-R-1772, Risø National Laboratory, Roskilde (Denmark).
[9] Rowley CW (2002). Modeling, simulation, and control of cavity flow oscillations, Ph.D. Thesis, California Institute of Technology.
[10] Rowley CW, Colonius T, Murray RM (2004). Model reduction for compressible flows using POD and Galerkin projection, Physica D. Nonlinear Phenomena 189(1–2):115–129.
[11] Bergmann M, Cordier L, Brancher JP (2005). Optimal rotary control of the cylinder wake using POD Reduced Order Model. Phys. Fluids 17, 097101:1–21
[12] Treuille A, Lewis A, Popovic Z (2006). Model reduction for real-time fluids. ACM Trans. on Graphics 25, 3, 826–834.
[13] Wicke M, Stanton M, Treuille A (2009). Modular bases for fluid dynamics. ACM Trans. on Graphics - Proceedings of ACM SIGGRAPH 2009.
[14] Holmes P, Lumley JL, Berkooz G (1996). Turbulence, Coherent Structures, Dynamical Systems and Symmetry. Cambridge Univ. Press, New York, 1996.
[15] Heggelund Y, Skaar IM, and Jarvis C (2012), Interactive design of wind farm layout using CFD and model reduction of the steady state RANS equation, 11th World Wind Energy Conference, Bonn, Germany. 3-5 July 2012.
[16] Pierella F, Krogstad PÅ, Sætran L (2014). Blind Test 2 calculations for two in-line model wind turbines where the downstream turbine operates at various rotational speeds. Renewable Energy 70 (2014) 62–77.
[17] Krogstad, P-Å and Eriksen, PE (2012). Blind test calculations of the performance and wake development for a model wind turbine. Renewable Energy 50 (2012) 225- 33.
[18] Khalil, M. and Sælen, L (2013). Near and far wake validation study for two turbines in line. EWEA2013, 4-7 February, Vienna, Austria.
[19] Sælen L, Khalil M, Melheim JA, Hansen T, Krogstad P-Å, Eriksen PE (2011). Near and far wake blind test study for a model turbine using BEM, AD and full rotor CFD. Conference proceedings, EWEA Offshore 2011, 29 November – 1 December 2011, Amsterdam, The Netherland.
[20] Heggelund Y, Khalil M, Jarvis C and Sælen L (2013). Interactive design of wind farm layout using CFD and model reduction, EWEA Offshore 2013, Frankfurt, Germany, 19-21 November 2013.
[21] Heggelund Y, Khalil M, Jarvis C (2014). Interactive design of wind farm layouts using CFD and model reduction, EWEA 2014, Barcelona, Spain, 10-13 March 2014.